Half-metallic density of states in Sr_2FeMoO_6 due to Hund's rule coupling

T. Saitoh,* M. Nakatake, and A. Kakizaki†
Photon Factory, Institute of Materials Structure Science, KEK, Tsukuba, Ibaraki 305-0801, Japan

H. Nakajima and O. Morimoto
Department of Materials Structure Science, Graduate University for Advanced Studies, Tsukuba, Ibaraki 305-0801, Japan

Sh. Xu
Department of Crystalline Materials Science, Nagoya University, Nagoya 464-8603, Japan

Y. Moritomo
Center for Integrated Research in Science and Engineering, Nagoya University, Nagoya 464-8601, Japan

N. Hamada
Department of Physics, Tokyo University of Science, Chiba 278-8510, Japan

Y. Aiura
National Institute of Advanced Industrial Science and Technology, Tsukuba, Ibaraki 305-8568, Japan
(Received 2 January 2002; published 19 July 2002)

We have investigated the electronic structure of Sr_2FeMoO_6 by photoemission spectroscopy and band-structure calculations within the local-density approximation+U (LDA+U) scheme. In valence-band photoemission spectra, a distinct double-peak feature has been observed near the Fermi level (E_F). A photon-energy dependence of the spectra and the LDA+U band-structure calculation have revealed that the first peak crossing E_F consists of the (Fe+Mo) $t_{2g\downarrow}$ states and the second peak well below E_F is dominated by the Fe $e_{g\uparrow}$ states. This clearly shows that only the down-spin states contribute to the E_F intensity, thus the half-metallic density of states (DOS) is realized. We point out that the observed half-metallic DOS can be attributed to the strong Hund's rule energy stabilization due to the high-spin $3d^5$ configuration at the Fe site.

DOI: 10.1103/PhysRevB.66.035112 PACS number(s): 71.20.Ps, 71.70.Gm, 75.30.Vn

I. INTRODUCTION

Colossal magnetoresistance (CMR) phenomena have been stimulating a large amount of research on the manganese oxides because of their potential applications to magneto-transport devices as well as their profound physics.[1] For industrial applications, however, one of the ideal properties is to work in a low magnetic field at room temperature (RT). In this sense, tunneling magnetoresistance (TMR) has been getting more attention than CMR. To realize such properties, the electronic structure should ideally have a half-metallic density of states (DOS) with a high Curie temperature (T_c). Although some of the manganites are half metallic,[2] many of them have low T_c and need a high magnetic field.

Recently, Kobayashi *et al.* reported that an ordered double perovskite Sr_2FeMoO_6 showed a large TMR, and they also predicted its half-metallic DOS like the manganites.[3] There have already been many studies on the family of the ordered double perovskites $ABB'O_6$ since the 1950's. Among them, iron-based compounds (Fe-Mo and Fe-Re) are special because they show metallic behavior with high ferrimagnetic T_c.[3–5] The ferrimagnetism (or *G*-type antiferromagnetism of Fe and Mo sites) of Sr_2FeMoO_6 has been proposed by Nakayama, Nakagawa, and Nomura using neutron diffraction.[6] Also, Nakagawa has confirmed the $Fe^{3+}(3d^5;t_{2g\uparrow}^3e_{g\uparrow}^2)$ configuration by Mössbauer spectroscopy.[7] Consequently, it is believed that this ferrimagnetism originates from the $Fe^{3+}(3d^5;t_{2g\uparrow}^3e_{g\uparrow}^2)$–$Mo^{5+}(4d^1;t_{2g\uparrow}^1)$ configuration, which produces $5-1=4\mu_B$.[3,4,6] However, the observed saturation moment by several groups has been always $3.1-3.2\mu_B$.[3,4,7–9] This low saturation moment has been attributed to a slight disorder of Fe-Mo ordering.[9,10]

On the other hand, García-Landa *et al.* have reported that $\mu_{Fe}=4.1\mu_B$ and $\mu_{Mo}=0.0\mu_B$.[11] This implies that the electron configuration may be close to the $Fe^{2+}(3d^6,t_{2g\uparrow}^3t_{2g\downarrow}^1e_{g\uparrow}^2)$–$Mo^{6+}(4d^0)$ configuration within a simple ionic model, although it is probably incompatible with the metallic behavior of this compound. From a recent Mössbauer measurement, Lindén *et al.* have claimed a valence-fluctuation state of $Fe^{2.5+}$.[12] Their result is supported by Chmaissem *et al.* who have obtained $\mu_{Fe}=4.3-4.4\mu_B$ from a neutron diffraction and a Mössbauer measurement.[13]

Thus the major problems on the electronic structure of Sr_2FeMoO_6 are (1) the half metallic DOS and (2) the valence of Fe and Mo ions (the origin of ferrimagnetism, in other words). Actually, those are closely related to each other because the calculated Fermi weight originates fairly in the Mo $4d$ $t_{2g\downarrow}$ states.[3,4,14,15]

Photoemission spectroscopy is suitable to investigate these issues; valence-band photoemission spectroscopy can reveal the valence-band electronic structure, and core-level photoemission spectroscopy can also provide important information about the valence states by observing chemical shifts of core levels. In particular, a Mo ion is known as an

ion which shows large chemical shifts with different valences. The direct method to confirm half-metallic DOS is spin-resolved photoemission (SRPES). However, it is very difficult to perform on bulk compounds. So far, there have been only two successful SPRES measurements on bulk oxides by Kämper *et al.* (CrO_2) (Ref. 16) and by Park *et al.* ($La_{0.7}Sr_{0.3}MnO_3$).[2]

Until now, the only photoemission study on Sr_2FeMoO_6 is by Sarma *et al.*[17] Surprisingly, they have found a very complicated Mo $3d$ core-level photoemission spectrum of Sr_2FeMoO_6, and it can never be attributed to a single valence such as Fe^{3+} or Fe^{2+}. From a cluster-model analysis, they have suggested the possibility of a negative $U_{\rm eff}$ at the Mo site.[17] In this paper, we present valence-band photoemission spectra of single crystals of Sr_2FeMoO_6 taken with synchrotron radiation light, and compare them with our band-structure calculations in detail. This is not as direct as SRPES, but it gives us sufficient information on the half-metallic DOS of this compound because of a double-peak feature which would be characteristic of the family of double perovskites.[18] Changing incident photon energies ($h\nu$), we extract information on the spectral distribution of the Fe $3d$ and Mo $4d$ states near E_F. Comparing the spectra with band-structure calculations, we will show that this distribution directly reflects the half-metallic electronic structure of this compound. We will also point out that the Hund's rule coupling at the Fe site should play an important role to realize the half-metallic electronic structure of this compound.

II. EXPERIMENT AND CALCULATION

High quality single crystals of Sr_2FeMoO_6 were grown by using the floating-zone method[19]. The site disorder was an order of 10% which would not seriously affect the microscopic electronic structure.[20] The experiments were performed at the beamline BL-11D of the Photon Factory (PF) using a Scienta SES-200 electron analyzer. The total energy resolution was about $50-90$ meV FWHM using $65-200$ eV photon energies. The chamber pressure was typically 2×10^{-10} Torr, and the temperature was about 20 K. The spectral intensity had been normalized by the total area of the full valence-band spectra and the near-E_F spectra were scaled to them.

Surface treatment is very important in photoemission experiments since the technique is highly surface-sensitive. It is common that the best way to obtain a clean surface of a bulk sample is to cleave the sample when it is cleavable. However, most three-dimensional samples including ours cannot be cleaved. In such a case, a common treatment is to scrape the sample using a diamond file. This is often successful for many compounds. For multinary oxides, however, it sometimes occurs that oxygen atoms easily come out during scraping due to the ultra-high vacuum, and then the surface may have a different composition. To obtain the best quality of surface, we fractured samples *in situ* at 20 K. The prepared surface was black and shining like a cleaved surface, but was rough enough to get angle-integrated spectra. For comparison, we also scraped samples with a diamond file.

Band-structure calculations were performed with the full-potential linearized augmented plane-wave (FLAPW) method[21] within the LDA+U scheme.[22,23] For effective Coulomb repulsions $U_{\rm eff}=U-J$, relatively small values (2.0 eV for Fe and 1.0 eV for Mo, respectively) were adopted. The experimental cubic lattice parameters ($d_{\rm Fe\text{-}O}=1.99$ Å and $d_{\rm Mo\text{-}O}=1.95$ Å) at 300 K (Ref. 4) were used.[24] The plane-wave cutoff energies were 12 Ry for the wave function, and 48 Ry for the charge density and the potentials. We took 19 k points in the irreducible Brillouin zone for the face-centered-cubic lattice.

III. RESULTS AND DISCUSSIONS

A. Band-structure calculations

First, we show the results of our LDA+U band-structure calculations in Fig. 1. As is seen in the figure, the top of the up-spin band is located at -0.8 eV while the down-spin band is crossing E_F, resulting in the half-metallic DOS. The down-spin conduction band crossing E_F is dominated by the Fe $3d-$Mo $4d$ $t_{2g\downarrow}$ states while the O $2p$ states have a smaller contribution. On the other hand, the up-spin band just below E_F is mostly due to the Fe $3d$ $e_{g\uparrow}$ and the O $2p$ states without any appreciable Mo $4d$ contribution. Hereafter, we simply denote the down-spin conduction band crossing E_F and the up-spin band just below E_F as a "Fe+Mo $t_{2g\downarrow}$ band" and a "Fe $e_{g\uparrow}$ band," respectively. The two sharp peaks between -2 and -4 eV in the Fe $3d$ up-spin band are due to the Fe $t_{2g\uparrow}$ states. Since those states overlap with the O $2p$ down-spin states, the Fe $t_{2g\uparrow}$ peaks may not be clear in our spin-integrated photoemission spectra. The major contribution to the $-4\sim-5.5$ eV region is from the O $2p$ states of up- and down-spin bands. There are considerable Fe $3d$ states between -5.5 eV and the bottom of the valence band in the up-spin band, too. This is due to the Fe $t_{2g\uparrow}$ and the Fe $e_{g\uparrow}$ bonding states which hybridize with the O $2p$ states. However, this Fe $3d$ weight would become relatively smaller in our spin-integrated spectra due to the large O $2p$ down-spin weight in the region, although the Fe weight has been observed in a similar compound by a Fe $3p$-$3d$ resonant photoemission measurement.[18]

Those generic features are consistent with the calculation using the generalized gradient approximation (GGA) by Kobayashi *et al.*[3] However, the top of the Fe $e_{g\uparrow}$ band in their calculation is quite close (≈-0.2 eV) to E_F compared with the present calculation. A calculation based on the linear muffin-tin orbital method using GGA was very similar to that of Kobayashi *et al.*[17,25] Since Kobayashi *et al.* used the almost identical lattice parameters to the present calculation,[24] the difference in our and their calculations should originate in a finite U first. In fact, before introducing U, the top of the Fe $e_{g\uparrow}$ band was very close to E_F in our calculation, too. This fact has been confirmed by other groups. For example, using the same lattice parameters as Kobayashi *et al.*, Fang, Terakura, and Kanamori obtained basically the same GGA DOS as Kobayashi *et al.*[14] In their LDA+U calculation, they adopted $U_{\rm eff}$ of 4 eV and 0 eV for Fe d and Mo d orbitals, respectively. Here, the $U_{\rm eff}$ of 4 eV for Fe is significantly larger than ours, and 0 eV for Mo in comparison to

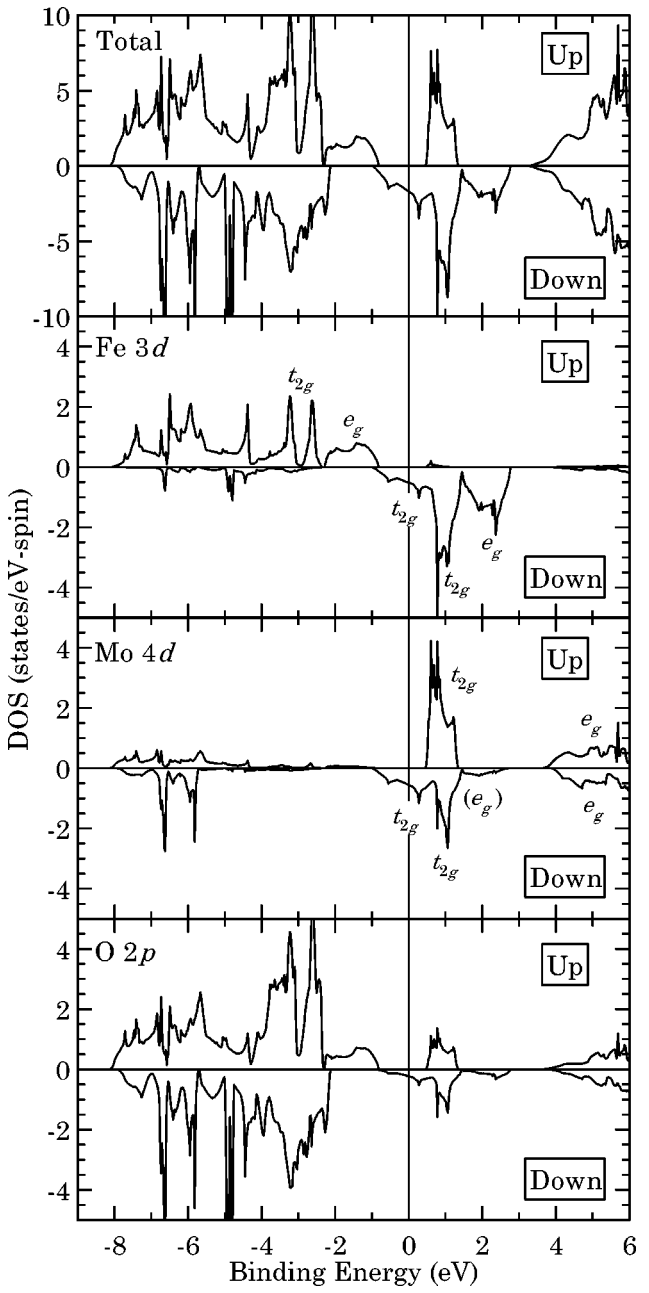

FIG. 1. Total and partial density of states of Sr_2FeMoO_6 calculated with LDA+U method. U_{eff} is 2.0 eV (Fe) and 1.0 eV (Mo). $d_{\text{Fe-O}}=1.99$ Å and $d_{\text{Mo-O}}=1.95$ Å.

our 1 eV enhances the effects of U on Fe sites. As a result, the top of the Fe $e_{g\uparrow}$ band moved to -1.2 eV. In addition, a large part of the $\text{Fe}_{\uparrow}$ spectral weight is strongly pulled down to -7.5 eV due to the large U_{eff}, forming a sharp and large peak at the bottom of the valence band. Wu compared local-spin-density approximation (LSDA) and LSDA+U with $U=4.5$ eV (Fe) and 1 eV (Mo), and obtained qualitatively the same results as Fang *et al.*[15] Kang *et al.* compared valence-band photoemission spectra of Ba_2FeMoO_6 with LSDA and LSDA+U calculations. The differences between LSDA and LSDA+U were very similar to the Sr_2FeMoO_6 case, and the LSDA+U calculation accounted for their Ba_2FeMoO_6 spectra being better than their LSDA.[18]

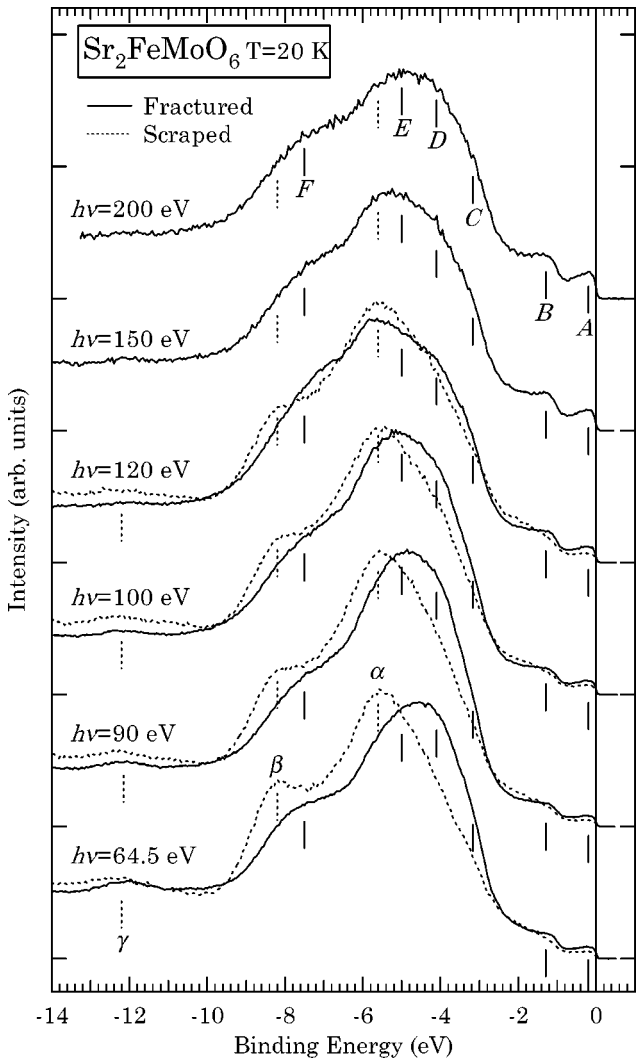

FIG. 2. Valence-band photoemission spectra of Sr_2FeMoO_6 at 20 K taken with several $h\nu$'s. Solid lines are the spectra of a fractured surface and dashed lines show the spectra of scraped surfaces.

The energy position of the Fe $e_{g\uparrow}$ band is a key to understanding near-E_F valence-band photoemission and optical-conductivity spectra. We will show later that neither the GGA/LDA nor the LDA+U with a large U calculation can reproduce the near-E_F spectra.

B. Photoemission spectra

Figure 2 shows valence-band photoemission spectra of Sr_2FeMoO_6 from a fractured surface (solid lines) and scraped (dotted lines) surfaces taken at 20 K. In the spectra of the fractured surface, one can easily observe four structures A (-0.20 eV), B (-1.30 eV), E (-5.0 eV), and F (-7.5 eV). Two shoulders C (-3.2 eV) and D(-4.1 eV), which are clearer in higher $h\nu$ (120 -200 eV), can also be observed. On the other hand, the spectra of scraped surfaces look rather different. A and B still can be seen but their intensity is quite suppressed. Moreover, D and E are not very clear while two structures α (-5.6 eV) and β (-8.2 eV) are enhanced instead. α is

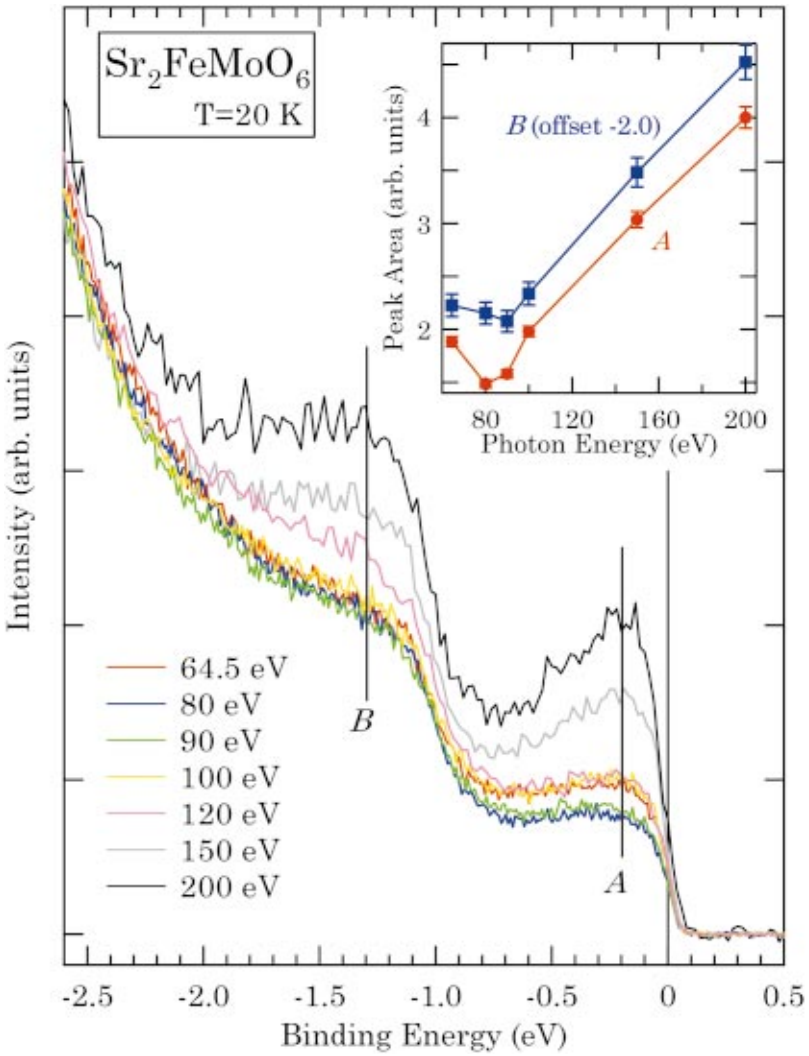

FIG. 3. (Color) Photoemission spectra of Sr_2FeMoO_6 near E_F region from a fractured surface at $T=20$ K taken with several $h\nu$'s. Inset: Integrated intensities of peak A (at -0.20 eV) and B (at -1.30 eV) in the ± 0.1 eV windows plotted as functions of photon energy. Note that the curve for B has an offset of -2.0 to compare with A in the same y scale.

actually observed as a shoulder in the 100, 150, and 200 eV spectra and as a peak in the 120 eV spectrum of the fractured surface, while it becomes very weak in the lower photon-energy spectra. β is hard to observe in the spectra of the fractured surface.

γ (-12.2 eV) has no intensity just after fracturing and grows with time, clearly indicating that it is related to surface-aging effects. Also, its intensity decreases from the lower to higher photon energies, and it is almost invisible in the 150 eV and 200 eV spectra. Considering that the intensity of the O $2p$ states is enhanced in the lower photon-energy region, γ is most probably due to oxygen states of suboxides on the surface. Here we note that the intensity of α and β also increases when γ grows due to surface aging, suggesting that they are related to the surface electronic structure too. In this sense, we can say that the fractured surface is more reliable than the scraped surface to investigate the bulk electronic structure of this compound. However, α is still obvious in the high $150-200$ eV photon energy and β will have its intensity in the spectra from the fractured surface, because even the high-photon-energy spectra have a relatively long tail in the bottom of the valence band. Hence, we believe that α and β should represent the surface electronic structure to some extent, but we also have the bulk component or the structures overlapping with α and β.

Comparing the raw calculational results in Fig. 1, we can immediately assign A and B to the Fe+Mo $t_{2g\downarrow}$ band and the Fe $e_{g\uparrow}$ band, respectively. C and D may correspond to the Fe $t_{2g\uparrow}$ states, although their energy positions are deeper than the theoretical positions by $\sim 0.6-0.9$ eV. For detailed analyses, however, we need to construct a theoretical spectrum and compare it with the experiment. This will be shown in Fig. 5. Before moving to this issue, let us see the near-E_F spectra first to observe the experimental distribution of the Mo $4d$ spectral weight in the near-E_F region.

Figure 3 shows near-E_F photoemission spectra of the fractured surface taken with several $h\nu$'s. The intensity of the structures A and B increases with $h\nu$. This indicates that considerable Fe $3d$ weight relative to the O $2p$ weight should exist in those structures because the photoionization cross section of the Fe $3d$ states relative to the O $2p$ states increases with $h\nu$ as shown in Fig. 4.[26] However, the behaviors of the spectral weight of A and B are quite different from each other. The inset shows the peak area of A and B vs $h\nu$. One can see that the spectral weight of A (red line) has a minimum at ~ 80 eV, while such a clear minimum is not

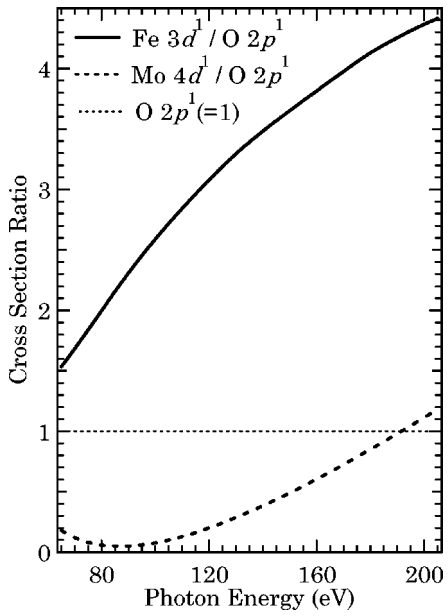

FIG. 4. Calculated photoionization cross section ratios of the Fe $3d$ (solid line) and Mo $4d$ (broken line) atomic states relative to the O $2p$ atomic state (per one electron of each state) after Yeh and Lindau.[26] The Mo $4d$ shows the Cooper minimum at $\sim 80-90$ eV.

observed in B (blue line). In fact, not only the spectral weight but also the line shapes of B at 80 eV and 90 eV are almost identical. On the other hand, Fig. 4 shows that the photoionization cross section ratio Mo $4d$/O $2p$ has a broad minimum near $\sim 80-90$ eV which is the Cooper minimum of the Mo $4d$ state. Hence the minimum of A should be interpreted as the Cooper minimum of the Mo $4d$ states. This is clearly demonstrating that A has a contribution from Mo $4d$ states whereas B has only an undetectably small contribution from those. This is in perfect agreement with both our and other groups' prediction of the band theories. It is, therefore, experimentally confirmed that the Fe $e_{g\uparrow}$ band and the Fe+Mo $t_{2g\downarrow}$ band are distributed from -2.2 eV to -0.9 eV and from -0.9 eV to E_F, respectively.

Tomioka *et al.* found a small peak at ~ 0.5 eV in their optical conductivity spectrum. Based on their band-structure calculation, they ascribed this peak to the Fe $e_{g\uparrow} \rightarrow$ Mo $t_{2g\uparrow}$ d-d absorption.[9] The above results, however, show that the Fe $e_{g\uparrow}$ states should be located far deeper than their interpretation. Besides, our band-structure calculation can reproduce the near-E_F photoemission spectrum, as shown below. Hence we infer that the 0.5 eV peak in the optical conductivity spectrum is not representing the half-metallic DOS unless the Fe $e_{g\uparrow}$ band has a long tail towards E_F.

C. Comparison between experiments and band-structure calculations

To compare experimental spectra and LDA+U band-structure calculations, we choose the 200 eV spectra because they are most bulk-sensitive. Figure 5 shows a comparison of the 200 eV spectra with the LDA+U calculation. The spin-integrated total DOS (gray area) includes only Fe d (white area), Mo d (black area), and O p (the other area) states because the other states have negligibly small intensity. The relative intensity of the three partial DOS was fixed to the calculated photoionization cross section.[26] A theoretical curve (solid line) was obtained by broadening the cross-section-corrected total DOS with a Gaussian due to the experimental resolution, and an energy-dependent Lorentzian due to the lifetime effect.[27] The background of the experimental spectra was subtracted.

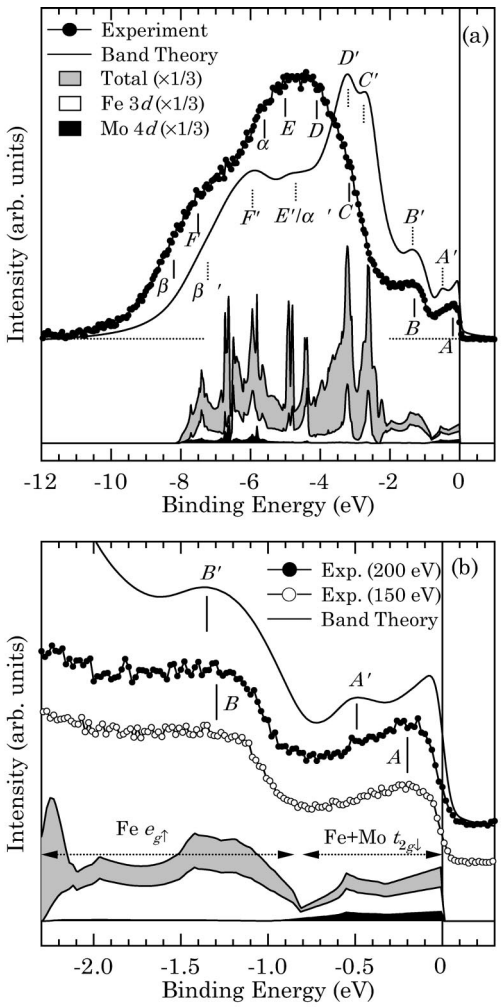

FIG. 5. (a) 200 eV photoemission spectrum of Sr_2FeMoO_6 at $T=20$ K (circles) compared to a theoretical curve using $d_{\text{Fe-O}}=1.99$ Å (solid curve). The experimental background has been subtracted. Vertical solid lines (A–F, α, β) denote the structures observed in Fig. 2 and the dotted lines (A'–F', α', β') are the corresponding features in the band theory. (b) 200 eV near-E_F spectrum is compared with the same LDA+U calculation. The 150 eV spectrum is also presented to show the location of A clearly. The experimental background of both spectra has been subtracted.

In (a), structures A'-F', α', and β' are observed in the theoretical curve. Now it is clear that the characteristic double-peak structure, A and B, is essentially reproduced in the theoretical curve as A' (Fe+Mo $t_{2g\downarrow}$) and B' (Fe $e_{g\uparrow}$). This double-peak structure cannot be reproduced by the GGA calculation by Kobayashi *et al.* because the Fe $e_{g\uparrow}$ band is too close to E_F in their calculation.[28] C' and D' are

due to the Fe $e_{g\uparrow}$ and the O $2p$ states. The O $2p$ contribution to C' and D' is rather large because of the overlapping O $2p$ down-spin states. It should be noted that C' and D' form a prominent (indeed, the largest) peak, and their energy position is quite different from the experimental C and D by $\sim$0.6–0.9 eV. E and α consist mainly of the O $2p$ nonbonding states which may be assigned to be a single structure E'/α'. Fe $t_{2g\uparrow}$ and Fe $e_{g\uparrow}$ bonding states contribute to F and β to some extent, respectively.

Figure 5(b) shows a comparison in the near-E_F region with a better signal-to-noise ratio. The energy position of the Fe+Mo $t_{2g\downarrow}$ band is in good agreement with the experiment. Moreover, the overall line shape of the band is also reproduced in the theoretical curve. However, the peak position in the experiment (A, -0.20 eV) is much closer to E_F than the theoretical position (A', -0.50 eV). Here, the 150 eV spectrum is also shown to see this -0.20 eV peak more clearly. Note that the peak at ~ -60 meV in the theoretical curve is not a real peak but one due to the Fermi edge. Consequently, the different energy position of A and A' can be interpreted as a band narrowing of the Fe+Mo $t_{2g\downarrow}$ band. Like the Fe+Mo $t_{2g\downarrow}$ band, the energy position of the Fe $e_{g\uparrow}$ band is in good agreement with the experiment. As for the line shape, however, only the lower binding-energy side of this band is well explained by the theoretical curve; a large tail of the Fe $t_{2g\uparrow}$ peaks, C' and D', is overlapping with the higher binding-energy side of the Fe $e_{g\uparrow}$ band, and this band is not as obvious as in the experiment.

The above comparison can be summarized into two points. (1) Our LDA+U calculation reproduces the energy position of the Fe+Mo $t_{2g\downarrow}$ and Fe $e_{g\uparrow}$ bands well, but the line shape of the Fe $e_{g\uparrow}$ band is not well reproduced due to the large Fe $t_{2g\uparrow}$ peaks. (2) Nevertheless, the theoretical Fe $t_{2g\uparrow}$ peaks are much closer to E_F (by $\sim$0.6–0.9 eV) than in the experiment. All the other states except the near E_F region are generally closer to E_F. As a result, the experimental valence-band width is wider by $\sim$1 eV. This is quite unique and unusual in the family of perovskite-type oxides because the valence-band width of those compounds is essentially reproduced by band-structure calculations.[29]

Within the LDA+U scheme, the above 1 eV shift must be explained by the relatively small value of $U_{\rm eff}$ for the Fe d states first. Indeed, the Fe $t_{2g\uparrow}$ states in the calculations of Fang *et al.* and Wu are located at $-3\sim -4$ eV in agreement with our experiment.[14,15] However, the top of the Fe $e_{g\uparrow}$ band is located at -1.2 eV in the calculation of Fang *et al.* with $U_{\rm eff}=4$ eV for Fe.[14] This is too deep compared to our experiment, and it becomes even worse (at -1.5 eV) in Wu's calculation with a similar $U_{\rm eff}$.[15] In addition, both calculations have a large peak at -7.5 eV due to the large $U_{\rm eff}$, which is not observed in the experimental spectra. Consequently, a large $U_{\rm eff}$ does not actually improve the band-structure calculations. Another explanation is a larger $U_{\rm eff}$ of the Fe t_{2g} states than the Fe e_g states. However, this would again produce an intense peak at the bottom of the valence band as shown by Solovyev *et al.* for the $LaFeO_3$ case.[30] Moreover, the shift of the whole valence band cannot be explained by this scenario.

Then, what is the origin of the 1 eV shift? In the crystal, the Fe (Mo) site is in the same environment as that of $SrFeO_3$ (nominally $3d^4$) [$SrMoO_3$ (nominally $4d^2$)]. However, since the effective charge-transfer (CT) energy $\Delta_{\rm eff}$ of $SrFeO_3$ is negative, the ground state of the Fe site (in $SrFeO_3$) is actually more like d^5L.[31,32] Here, L and $\underline{L}$ denote an O $2p$ ligand electron and hole, respectively. By contrast, it is known that Mo ions are stable in higher oxidation states. Hence Mo^{+4} strongly tends to lose an electron: $4d^2 \rightarrow 4d^1\underline{L}$.[33] Then $3d^5\underline{L}+4d^1\underline{L}$ naturally turns out to be the $3d^5+4d^1$ configuration (before the Fe-Mo hybridization is switched on). This situation realizes the same electronic configuration at the Fe site as in $LaFeO_3$ ($3d^5$) which is a large-gap insulator.

This d^5 configuration under the cubic symmetry is very special. Within the Hartree-Fock (HF) approximation, the d-d energy gap of the d^5 configuration is an order of $U+4J$ while it is much smaller ($\sim U-J$) in the other electron configurations.[34] This is the Hund's rule energy stabilization in the d^5 configuration and the major origin of the large $E_{\rm gap}$ of d^5 compounds.[32] However, $LaFeO_3$ is actually a CT-type insulator whose $E_{\rm gap}$ is also controlled by $\Delta_{\rm eff}$.[32] Thus in the $3d^5$ compounds the large $E_{\rm gap}$ is determined by both the strong Hund's rule coupling and $\Delta_{\rm eff}$, but not by the simple Coulomb repulsion. Therefore, just a large Coulomb repulsion in the Fe states cannot account for the discrepancy between the LDA theory and the experiment.

It is worth noting that the local Fe DOS in the calculations with a large $U_{\rm eff}$ are very similar to those of the unrestricted HF calculations on $LaFeO_3$ by Mizokawa and Fujimori,[35] in which the Fe DOS also have an intense peak at the bottom of the valence band. This similarity suggests that a large $U_{\rm eff}$ almost completely corrects the self interaction and hence recovers the effects of the nonlocal exchange potential which has been neglected in LDA but is fully taken into account in the HF approximation. In this sense, what is lacked in our calculation (and LDA) is not a large Coulomb repulsion but the appropriate (not just nonlocal) exchange interaction (and of course the electron correlation effects). For $LaFeO_3$, an FeO_6^{-9} cluster-model calculation gives a peak-to-peak $E_{\rm gap}$ of $\sim$5 eV (Ref. 32) and optical and photoemission-inverse photoemission $E_{\rm gap}$'s of $\sim$2 eV have been reported.[36,37] Then, a peak-to-peak gap of $\sim$1–2 eV below E_F should be expected for the $Fe_\uparrow$ band in Sr_2FeMoO_6. It is indeed observed as feature B (located at -1.3 eV) in our experimental spectra. On the other hand, the bottom of the valence band in self-energy-corrected HF calculations has generally a smaller spectral weight than HF calculations, and a long tail appears in the higher-binding energy region instead.[38] Hence, the lack of the large peak at the bottom of the valence band in our experiment can probably be explained by the above electron-correlation effects.

The electronic structure of Sr_2FeMoO_6 is schematically summarized in Fig. 6. (a) depicts the DOS of the Fe $3d^5$ + Mo $4d^1$ ionic state without the Fe-Mo hybridization. The Fe up-spin states are already pulled down and forming an energy gap due to the strong Hund's rule coupling, while the Mo t_{2g} states generate the Fermi surface. (b) shows the

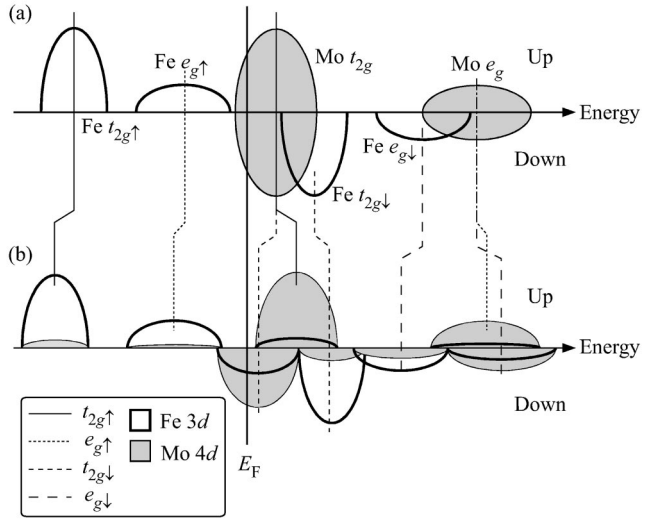

FIG. 6. Schematic electronic structure of Sr_2FeMoO_6 (a) in the ionic state, and (b) in the real Fe-Mo hybridized state (via oxygen). Solid and broken lines denote the symmetry of those hybridizations.

DOS with the Fe-Mo hybridization via oxygen sites. The occupied Fe up-spin states are further pushed down due to the hybridization, and the Mo t_{2g} up- and down-spin states split due to different hybridization strength.[39] Thus the strong Hund's rule coupling of the d^5 configuration and the different hybridization strength between up- and down-spin channels cooperatively work to realize the half-metallic DOS in this compound.

Finally we compare the electronic structure of this compound and the magnetoresistive manganites. From our results, as well as the results by other groups, it is shown that the $3d^5$ Fe up-spin states are well localized and behave as a large local spin of $S=5/2$. Here we note that this spin almost purely originates from the Fe states because we have observed no appreciable Mo weight in structure *B*. The Mo-Fe t_{2g} down-spin electrons move around and *antiferromagnetically* couple to the local spins. This situation is a (large) local spin + charge carriers, namely the double exchange (DE) scheme as pointed out by Kang *et al.*[18] The difference from the manganites is merely that the charge carriers are inevitably in the down-spin band simply because the up-spin states are fully occupied. The local spin of this system ($S=5/2$) is larger than that of the manganites ($S=3/2$). This would explain the higher T_c than the manganites. Nevertheless, Sr_2FeMoO_6 does not show CMR. The reason is probably that Sr_2FeMoO_6 is a very typical DE compound like a heavily doped manganite, for example $La_{0.6}Sr_{0.4}MnO_3$. The DE theory predicts a finite Fermi weight even above T_c and hence does not predict any metal-insulator transitions (MIT).[40] In accordance with this, both compounds have a relatively large Fermi weight and do not show MIT either. In contrast, all the CMR manganites show sharp MIT and have vanishingly small Fermi weight, or in other words, a pseudogap.[41] Therefore, even though the DE can explain the MR effects to some extent, it cannot explain *colossal* magnetoresistance. The essence of CMR is MIT and the first reason would probably be the pseudogap. In this sense, the $3d^5$ "half-filled" Sr_2FeMoO_6 is a good reference to examine how the DE theory appears in real compounds.

IV. CONCLUSIONS

In conclusion, we have investigated the electronic structure of bulk Sr_2FeMoO_6 by photoemission spectroscopy and LDA+U band-structure calculations. In the photoemission spectra, we have observed a double-peak structure near E_F which is characteristic of metallic double perovskites. The band-structure calculations have shown that this double-peak structure cannot be reproduced by LDA/GGA nor LDA+U with a large U. Making use of the Mo 4d Cooper minimum and comparing with the LDA+U calculations, we have extracted the distribution of the Fe 3d and Mo 4d states in the double-peak structure; the first peak crossing E_F consists of (Fe+Mo) $t_{2g\downarrow}$ states whereas the second peak's lower ($\sim$1.3 eV) E_F has only Fe $e_{g\uparrow}$ states, demonstrating that only the down-spin states contribute to the E_F intensity. We have pointed out that the observed half-metallic DOS can be attributed to the strong Hund's-rule energy stabilization due to the high-spin $3d^5$ configuration at the Fe site.

ACKNOWLEDGMENTS

The authors would like to thank T. Kikuchi for technical supports in the experiments. Part of this work was done under the approval of the Photon Factory Program Advisory Committee (Proposal No. 00G011). This work was supported by a Grant-in-Aid for Scientific Research from the Ministry of Education, Science and Culture, Japan.

*Corresponding author. Present address: Department of Applied Physics, Tokyo University of Science, Shinjuku, Tokyo 162-8601, Japan.

†Present address: Institute for Solid State Physics, University of Tokyo, Kashiwa, Chiba 277-8581, Japan.

[1] For reviews, see *Colossal Magnetoresistance, Charge Ordering and Related Properties of Manganese Oxides*, edited by C. N. R. Rao and B. Raveau (World Scientific, Singapore, 1998); *Colossal Magetoresistive Oxides* edited by Y. Tokura (Gordon and Breach, New York, 2000).

[2] J.-H. Park *et al.*, Nature (London) **392**, 794 (1998).

[3] K.-I. Kobayashi, T. Kimura, H. Sawada, K. Terakura, and Y. Tokura, Nature (London) **395**, 677 (1998).

[4] Y. Moritomo, Sh. Xu, A. Machida, T. Akimoto, E. Nishibori, M. Takata, and M. Sakata, Phys. Rev. B **61**, R7827 (2000).

[5] K.-I. Kobayashi, T. Kimura, Y. Tomioka, H. Sawada, K. Terakura, and Y. Tokura, Phys. Rev. B **59**, 11 159 (1999).

[6] S. Nakayama, T. Nakagawa, and S. Nomura, J. Phys. Soc. Jpn. **24**, 219 (1968).

[7] T. Nakagawa, J. Phys. Soc. Jpn. **24**, 806 (1968).

[8] M. Itoh, I. Ohta, and Y. Inaguma, Mater. Sci. Eng., B **41**, 55 (1996).

[9] Y. Tomioka, T. Okuda, Y. Okimoto, R. Kumai, K.-I. Kobayashi, and Y. Tokura, Phys. Rev. B **61**, 422 (2000).

[10] A. S. Ogale, S. B. Ogale, R. Ramesh, and T. Venkatesan, Appl. Phys. Lett. **75**, 537 (1999).
[11] B. García-Landa, C. Ritter, M. R. Ibarra, J. Blasco, P. A. Algarabel, R. Mahendiran, and J. García, Solid State Commun. **110**, 435 (1999).
[12] J. Lindén *et al.*, Appl. Phys. Lett. **76**, 2925 (2000).
[13] O. Chmaissem, R. Kruk, B. Dabrowski, D. E. Brown, X. Xiong, S. Kolesnik, J. D. Jorgensen, and C. W. Kimball, Phys. Rev. B **62**, 14 197 (2000).
[14] Z. Fang, K. Terakura, and J. Kanamori, Phys. Rev. B **63**, 180407 (2001).
[15] Hua Wu, Phys. Rev. B **64**, 125126 (2001).
[16] K. P. Kämper, W. Schmitt, G. Güntherodt, R. J. Gambino, and R. Ruf, Phys. Rev. Lett. **59**, 2788 (1987).
[17] D. D. Sarma, Prya Mahadevan, T. Saha-Dasgupta, Sugata Ray, and Ashwani Kumar, Phys. Rev. Lett. **85**, 2549 (2000).
[18] J.-S. Kang, H. Han, B. W. Lee, C. G. Olson, S. W. Han, K. H. Kim, J. I. Jeong, J. H. Park, and B. I. Min, Phys. Rev. B **64**, 024429 (2001).
[19] Y. Moritomo, Sh. Xu, T. Akimoto, A. Machida, N. Hamada, K. Ohoyama, E. Nishibori, M. Takata, and M. Sakata, Phys. Rev. B **62**, 14 224 (2000).
[20] The site disorder realizes Fe-O-Fe and Mo-O-Mo couplings. Those should affect the macroscopic magnetization to some extent because $SrFeO_3$ (Fe-O-Fe) is a screw antiferromagnet. [T. Takeda, Y. Yamaguchi, and H. Watanabe, J. Phys. Soc. Jpn. **33**, 967 (1972)]. However, the electronic configuration would still be $3d^5$ in this case due to the negative effective-charge-transfer energy Δ_{eff} of this compound.[31,32] Hence the site disorder will not significantly affect the local electronic structure, particularly the energy gain due to Hund's rule coupling at the Fe sites.
[21] O. K. Andersen, Phys. Rev. B **12**, 3060 (1975); T. Takeda and J. Kubler, J. Phys. F: Met. Phys. **9**, 661 (1979).
[22] P. Hohenberg and W. Kohn, Phys. Rev. **136**, B864 (1964); W. Hohn and L. J. Sham, *ibid.* **140**, A1133 (1965); S. H. Vosko, L. Wilk, and M. Nusair, Can. J. Phys. **58**, 1200 (1980).
[23] V. I. Anisimov, J. Zaanen, and O. K. Andersen, Phys. Rev. B **44**, 943 (1991); V. I. Anisimov, F. Aryasetiawan, and A. I. Lichtenstein, J. Phys.: Condens. Matter **9**, 767 (1997); I. Solovyev, N. Hamada, and K. Terakura, Phys. Rev. B **53**, 7158 (1996).
[24] There have been a couple of reports on the crystalline structure. Itoh *et al.*,[8] Kobayashi *et al.*,[3] and Moritomo *et al.*,[19] have reported a slightly tetragonal lattice, although their $d_{\mathrm{Fe\text{-}O}}$ and $d_{\mathrm{Mo\text{-}O}}$ are a little different from each other. On the other hand, García-Landa *et al.*[11] and Moritomo *et al.*[4] have reported a cubic lattice. Recently, Chmaissem *et al.*[13] have observed a structural phase transition from cubic to tetragonal with decreasing temperature by neutron diffraction, showing that the system is almost cubic. $d_{\mathrm{Fe\text{-}O}}$ and $d_{\mathrm{Mo\text{-}O}}$ from Ref. 4 and Ref. 13 are very close to each other. Moreover, Kobayashi *et al.* have theoretically optimized $d_{\mathrm{Fe\text{-}O}}$ and $d_{\mathrm{Mo\text{-}O}}$, obtaining quite similar numbers to the above two. Therefore, we believe that the $d_{\mathrm{Fe\text{-}O}}$ and $d_{\mathrm{Mo\text{-}O}}$ based on Refs. 3, 4, and 13 are the most reliable for the real lattice.
[25] D. D. Sarma, Current Opin. Solid State & Mater. Sci. **5**, 261 (2001).
[26] J. J. Yeh and I. Lindau, At. Data Nucl. Data Tables **32**, 1 (1985).
[27] T. Saitoh, T. Mizokawa, A. Fujimori, M. Abbate, Y. Takeda, and M. Takano, Phys. Rev. B **56**, 1290 (1997).
[28] Since their result was very similar to our previous calculation,[19] we have checked how their result can explain our experiment using our previous calculation.
[29] D. D. Sarma, N. Shanthi, S. R. Barman, N. Hamada, H. Sawada, and K. Terakura, Phys. Rev. Lett. **75**, 1126 (1995).
[30] I. Solovyev, N. Hamada, and K. Terakura, Phys. Rev. B **53**, 7158 (1996).
[31] A. E. Bocquet, A. Fujimori, T. Mizokawa, T. Saitoh, H. Namatame, S. Suga, N. Kimizuka, Y. Takeda, and M. Takano, Phys. Rev. B **45**, 1561 (1992).
[32] T. Saitoh, A. E. Bocquet, T. Mizokawa, and A. Fujimori, Phys. Rev. B **52**, 7934 (1995).
[33] This may be related to the negative U_{eff} at the Mo site suggested by Sarma *et al.*[17]
[34] Assuming that all the configurations are high-spin states, which is usually the case.
[35] T. Mizokawa and A. Fujimori, Phys. Rev. B **54**, 5368 (1996).
[36] T. Arima, Y. Tokura, and J. B. Torrance, Phys. Rev. B **48**, 17 006 (1993).
[37] A. Chainani, M. Mathew, and D. D. Sarma, Phys. Rev. B **48**, 14 818 (1993).
[38] T. Mizokawa and A. Fujimori, Phys. Rev. B **53**, R4201 (1996).
[39] J. Kanamori and K. Terakura, J. Phys. Soc. Jpn. **70**, 1433 (2001).
[40] K. Kubo and N. Ohata, J. Phys. Soc. Jpn. **33**, 21 (1972); K. Kubo *ibid.* **33**, 929 (1972).
[41] D. S. Dessau, T. Saitoh, C.-H. Park, Z.-X. Shen, P. Villella, N. Hamada, Y. Moritomo, and Y. Tokura, Phys. Rev. Lett. **81**, 192 (1998); T. Saitoh, D. S. Dessau, Y. Moritomo, T. Kimura, Y. Tokura, and N. Hamada, Phys. Rev. B **62**, 1039 (2000).